# Influence of boundary conditions and component size on electricity demand in solar thermal and heat pump combisystems.

Stefano Poppi*[1,2], Chris Bales[1], Michel Y. Haller[3], Andreas Heinz[4]

[1]Solar Energy Research Center (SERC), Dalarna University College, S-79188 Falun, Sweden

[2]Department of Energy Technology, KTH, SE-100 44 Stockholm, Sweden

[3]Institut für Solartechnik SPF, University of Applied Sciences HSR, Oberseestr. 10, 8640 Rapperswil, Switzerland

[4]Institute of Thermal Engineering, Graz University of Technology, Inffeldgasse 25b, A-8010 Graz, Austria

*Corresponding author. Tel.: +46 23 77 87 46; Fax: +4623778701; E-mail address: spo@du.se

This is an author-produced version of a paper accepted for publication in the Applied Energy journal (Elsevier) in January 2016. This version has been peer-reviewed, but does not include the final publisher proof corrections, published layout, or pagination.
For the official version, please refer to doi:10.1016/j.apenergy.2015.10.190

**Abstract**

Solar thermal and heat pump combisystems are used to produce domestic hot water (DHW) and space heating (SH) in dwellings. Many systems are available on the market. For an impartial comparison, a definite level of thermal comfort should be defined and ensured in all systems. This work studied the influence of component size on electricity demand for a state of the art solar thermal and heat pump system. A systematic series of parametric studies was carried out by using TRNSYS to show the impact of climate, load and size of main components as well as heat source for the heat pump. Penalty functions were used to ensure that all variations provided the same comfort requirements. Two reference systems were defined and modelled based on products on the market, one with ambient air and the other with borehole as heat source for the heat pump. The results show that changes in collector area from 5 to 15 $m^2$ result in a decrease in system electricity of between 305 and 552 kWh/year. Changes in heat exchanger size for DHW preparation were shown to give nearly as large changes in electricity use due to the fact that the set temperature in the store was changed to give the same thermal comfort in all cases. Decrease in heat pump size was shown to give a decrease in electricity use for the ASHP in the building with larger heat demand while it increased or had only a small change for other boundary conditions. Heat pump losses were shown to be an important factor highlighting the importance of modelling this factor explicitly.

**Keywords**

Solar Combisystem, heat pump, component size, simulation

**Nomenclature**

| | |
|---|---|
| ASHP | air source heat pump |
| AC45 | ASHP, house with insulation standard SFH45 and with Carcassonne climate |
| AC100 | ASHP, house with insulation standard SFH100 and with Carcassonne climate |
| AZ45 | ASHP, house with insulation standard SFH45 and with Zurich climate |
| AZ100 | ASHP, house with insulation standard SFH100 and Zurich climate |
| CA | Carcassonne |
| DHW | domestic hot water |
| FSC | Fractional Solar Consumption |
| GSHP | ground source heat pump |
| GC45 | GSHP, house with insulation standard SFH45 and with Carcassonne climate |
| GC100 | GSHP, house with insulation standard SFH100 and with Carcassonne climate |
| GZ45 | GSHP, house with insulation standard SFH45 and with Zurich climate |
| GZ100 | GSHP, house with insulation standard SFH100 and Zurich climate |
| HP | heat pump |
| I | annual solar radiation [kWh/year] |
| $\dot{m}$ | mass flow rate [kg/s] |
| p | pressure [Pa] |
| Q | annual thermal energy [kWh/year] |
| SFH | single family house |
| SH | space heating |
| SPF | seasonal performance factor |
| T | temperature [°C] |
| W | annual electrical energy consumption [kWh/year] |
| ZH | Zurich |

*Subscript*

| | |
|---|---|
| *Ctr* | *controller* |
| *cpr* | *compressor* |

| | |
|---|---|
| *DHW* | *domestic hot water* |
| *dist* | *circulation pumps* |
| *EH* | *auxiliary electrical heater* |
| *el* | *electrical* |
| *HP* | *heat pump* |
| *LOSS* | *losses* |
| *pen* | *penalties* |
| *S* | *south* |
| *SC* | *solar collector* |
| *SH* | *space heating* |
| *SHP* | *solar heat pump* |
| *Start/stop* | *heat pump start and stop* |
| *tot* | *total* |
| *V* | *system variation* |
| *45* | *tilt angle of solar collector* |

## 1. Introduction

The use of solar thermal and heat pump combisystems is widespread in the market of space heating (SH) and hot water preparation (DHW) for single family houses. Recent studies of the state of art in Europe [1, 2] have shown that solar collector can be used either in parallel or in series with heat pump. In parallel systems, both solar collector and heat pump provide heat for the loads either directly or via the store, while in series, heat from the solar collector is used indirectly as the heat source for a heat pump evaporator. Haller et al. [3] studied the use of solar heat for the evaporator and concluded that this was beneficial only when radiation on the collector was below certain threshold value, which was shown to be dependent on the efficiency of collector and heat pump as well as operating temperature levels.

Seasonal performance factor (SPF) of the whole system increases significantly when solar thermal is added in parallel with heat pumps, either air source (ASHP) or ground source (GSHP), because part of the heating demand is covered by the solar collectors. The ratio of heat delivered to electricity use is higher for solar collectors than for heat pumps. The increase in SPF is largely dependent on the heat load (total heat demand, share of DHW, and distribution over the year) as well as on the solar resource that is available (climate and collector area and orientation) [4].

The SPF of ASHP itself may not always be enhanced by adding solar thermal and this is shown in [5, 6]. It was found that solar covered part of the thermal load during the time when the ASHP worked efficiently, i.e. spring and summer periods. Moreover, the system SPF was better in the solution with solar because the heat pump ran for a shorter time at high sink temperatures. In [6] results in terms of absolute electricity revealed higher savings for ASHP rather than for GSHP. This was due to the higher electricity use of the ASHP compared to the GSHP in the system used for comparison. Indeed, ASHP tend to use more electricity compared to GSHP and this for two main reasons. The first reason is that ASHP has a higher temperature difference between source and sink during the time of year when most of the heat is delivered. The second reason is that ASHP has larger losses than GSHP mostly for defrosting the ice that forms on the surface of the air heat exchanger (evaporator).

Research on solar combisystems is active and many studies are available in literature [7-30], with many including heat pumps as the auxiliary heat source. Colclough and McGrath in [7] presented a case study of a passive house with a solar thermal combisystem with a seasonal storage. Asaee et al. in [9] proposed a system configuration that is suitable for the heating and cooling of Canadian residential houses and the influence of climate, collector area and storage capacity on system performance was investigated. The solar field consisted of 24 $m^2$ flat plate collectors and served a 3$m^3$ storage tank and a 0.2 $m^3$ pre-heated DHW tank. Results showed that the change in collector area had bigger impact than the change in storage size on annual solar fraction and for all climates investigated. Annual solar fraction ranged from 0.63 for

15 $m^2$ collector area and in Montreal to 0.86 for 36 $m^2$ in Edmonton. Kaçan et al. in [12,17] investigated small solar combisystems in Turkey. Collector area was 2.6 $m^2$ and the storage tank had a volume of 300L. The auxiliary heat source was a 2kW electrical heater placed in the storage tank. Energetic and exergetic efficiencies for each component and for the whole system were derived. One conclusion was that tank volume is an important parameter to use the gained energy effectively and avoid excessive energy production. Leconte in [18] used artificial neural network (ANN) for the characterization of solar systems combined with boilers. A simulation model was verified by means of measurements under two different tests conditions. Experimental results showed small differences (lower than 2% in both tests) between measured data and numerical data in auxiliary energy use and in space heating energy. Much larger differences were shown for the captured solar energy due to that the model overestimated solar gains. Lundh et al. in [22] investigated the influence of the store geometry on the performance of the solar heating system and compared the performance of a storage tank with an internal auxiliary volume to the performance of a solution with an external unit. Maximum fractional savings were found at height to diameter ratios of 2 to 4 that includes the range recommended for commercial store. The comparison showed that a solution with an internal volume led to higher fractional energy savings for almost any volume and geometry configuration. Thür in [23] studied a solar combisystem combined with a condensing natural gas boiler. Simulations were carried out for the climate of Stockholm and for two system sizes, a small one (6 $m^2$ solar collector and a 300L storage tank) and a large one (20 $m^2$ solar collector and a 1000L storage tank) and results were compared to those of a traditional boiler system with no solar. Results showed larger energy savings for the large system. Spur et al. in [24] analysed the effects of common draw-off profiles on store performance and three realistic daily profiles, which were based on field measurements, were developed, concluding that it is important to have realistic DHW draw-off profiles for systems with internal heat exchangers for preparation of DHW. Jordan and Vajen [29] also found that realistic DHW profiles are important and derived a methodology to make synthetic but realistic profiles based on a statistical approach. This method was implemented in a tool called DHWcalc that was then used to derive the DHW profiles used in IEA-Task 26 simulations [28]. Andersen et al. in [25] and in [27] investigated the thermal performance of many Danish systems. They concluded that it is important to keep the auxiliary heated volume as small as possible and to keep the temperature of the auxiliary volume as low as possible. Moreover, it was found that the best performing system for a solar fraction from 4% to 15% and low DHW discharge energy was a system with a tank in tank heat storage, while for high DHW discharge energy, a system with a heat exchanger spiral for the SH system performed better. Lund in [26] studied the dimensioning of solar combisystem with focus on the size of solar collector and thermal storage. An analytical model was derived to study the effects of different sizing parameters and driving factors. Results were compared to those of numerical simulations showing reasonable accuracy. The

conclusion was that the increasing of collector area is not justified in the case with low energy buildings and in regions with high solar irradiation, i.e. southern Europe. Furthermore, increase of the size of the storage tank far beyond the daily capacity was proved not to be justified in solar combisystems.

The use of heat pump in combination with a solar collector was studied in [8,10,11,13,14,16,19,20,21] and a large variety of heat pump configuration was shown in those works. Much is summarized in a handbook that is a result of the collaboration within IEA SHC Task 44 / HPP Annex 38 (T44A38) “Solar and Heat Pump Systems” [30]. Schimpf and Span in [8] studied a solar thermal system combined with a reversible GSHP together with an Organic Rankin Cycle (ORC). The ORC was used for recharging the ground when a predefined temperature in the storage tank was reached. Bertram et al. in [10] simulated different solar assisted GSHP systems and the impact of solar on system efficiency and on the possible shortening of the ground heat exchanger was evaluated. Carbonell et al. in [11] studied the potential benefit of combining solar thermal with heat pump systems for several European cities. The main conclusion was that the SPF increases when a solar thermal system is added for both ASHP and GSHP. Li et al. in [13] investigated the influence of storage factor, collector area and dead-band temperature of an air source heat pump combisystem on system performance. The solar field was designed to meet the DHW requirement and part of space heating load when the ambient air temperature turns below the dead-band temperature of the air-to-water heat pump. The main conclusion was that a properly designed system can operate effectively and significantly reduce energy consumption compared with the traditional system used in cold climate buildings. Deng et al. in [14] and in [20] simulated the use of CO2 as refrigerant medium of a heat pump in solar combisystems. Dott et al. in [16] evaluated several configurations of solar system combined with heat pump with the focus on the use of solar irradiation. They showed that the focus on direct solar generated heat, with larger share for the building with lower space heat demand, leads to the smallest electricity consumption and thus highest system efficiency. Sterling and Collins in [19] studied the feasibility of indirect solar assisted heat pump by comparing to a traditional solar domestic hot water (SDHW) system and to an electric domestic hot water (DHW) system. They concluded that there is potential for the use of heat pumps to assist solar domestic water heating systems to increase the performance of SDHW systems. Kjellsson et al. in [21] focused on systems with GSHP combined with solar thermal analysing different system alternatives in order to find the best strategies in terms of system design and operation. They concluded that the optimal design for reducing the use of electricity is when solar heat produces DHW during summertime and recharges the borehole during wintertime. The literature survey shows that a lot of research has been carried out, but that there is no structured study that includes both ASHP and GSHP for a wide range of boundary conditions. Thus this study was planned to fill this gap, using parametric studies for the size of the main components to highlight the differences between state-of-the-art ASHP and GSHP systems for different conditions and for different system sizes.

The key-figures that were used in the aforementioned studies to compare system results were the solar fraction [9,13,14,19,26], the electricity use and the energy use [8,12,15,16,17,20,21,23,24], energy savings [7,11,16] and fractional energy savings [18,22] and SPF [10,11,15,21]. When comparing systems with such key figures, it is important to ensure that the systems provide the same level of comfort, thus same standard to the user. One method for ensuring this is the concept of penalty functions, which was introduced within the IEA SHC Task26 programme, and is reported in [28]. If the investigated heating system is not able to fulfil the user demand for the room temperature or DHW supply temperature, an additional energy demand, the penalty, is calculated and included as an auxiliary energy demand of the heating system [28]. Only few of the aforementioned studies with heat pumps [10,15,30] included the penalties in the definition of annual energy demand and SPF, although other, less rigorous approaches, have been used in some of the studies to ensure the same level of energy supply to the user.

The aim of this study was to investigate in a systematic way the impact on system performance of the size of the main components in solar thermal heat pump combisystems, ensuring in all cases the same level of comfort to the end user by using penalty functions. In order to make the study more general and thus complete, the two main types of heat pumps, air and ground source, are simulated with Trnsys17 [31] for two climates and two loads. Heat pumps were modelled in detail by means of a semi-physical model and main parameters were derived from measurement a heat pump that was available in the market at the time of the study. The system design is state of the art for what was available on the market at the time of the study.

This investigation has been carried out within the frame of the European Union's Seventh Framework Program FP7/2007-2011 in a project called MacSheep [32].

## 2. Methodology

This study was carried out in Trnsys17 for two climates, Zurich (ZH) and Carcassonne (CA), as well as two houses with different insulation standards (SFH45 and SFH100) in order to get a large range of space heating loads as well as solar resource. The fractional solar consumption (FSC) is the ratio of the usable irradiation available on the collector field to the useful heat delivered [28] calculated for a complete year, with values being between 0 and 1. It has been shown to be correlated with the fractional energy savings of solar combisystems in general [28] as well as solar combisystems with heat pumps [30]. The FSC for the combination of the chosen two climates and two house standards ranged from 0.33 to 0.76 for the default system size, and from 0.22 to 0.91 for the collector range used in the sensitivity analysis. Thus the paper presents results for a very wide range of FSC values and thus possible energy savings. Additionally the heat distribution systems for the two houses are sized differently, with the SFH45 house having design temperatures representing floor heating while for the SFH100 house design temperatures are for radiators and thus higher. The model parameters for the building models were the same as those defined for IEA SHC Task 44 / HPP Annex 38 (T44A38) “Solar and Heat Pump Systems” and shown in [33]. Climate data are shown in Table 1. The average ambient temperature is 4 ºC higher in Carcassonne than Zurich and the design outside ambient temperature is 5 ºC higher. The radiation on the 45° inclined south facing surface is also 255 kWh/(m$^2$·year) higher in Carcossonne. Details of DHW load with two-minute time step are reported in [34]. A realistic DHW profile was chosen with many variation in flow rates and large number of discharges with small flow rates. The profile was derived for a family of four people with the program DHWcalc, which uses statistical probabilities of different types of discharge and their flow rates and duration, and which is based on the theory described in [28].

Table 1 Climata data for Carcassonne and Zurich.

| **Location** | **Lat.** | **Alt. [m]** | **Design Outside Ambient Temperature [°C]** | **Average Outside Ambient Temperature [°C].** | **$I_{tot,45S}$ [kWh/m$^2$·year]** |
|---|---|---|---|---|---|
| Carcassonne | 43.22° N | 130 | -5.0 | 13.2 | 1561 |
| Zurich | 47.37° N | 413 | -10.0 | 9.1 | 1306 |

A summary of the key figures for the four combinations is shown in Table 2. The space heating load in Carcassonne is less than half that in Zurich and the annual DHW discharge energy is circa 350 kWh/year smaller.

Table 2 Key figures for the loads used in the study.

| | ***ZH45*** | ***ZH100*** | ***CA45*** | ***CA100*** |
|---|---|---|---|---|
| Supply temperature for DHW [°C] | 45 | 45 | 45 | 45 |
| Cold water temperature for DHW [°C] | 10 | 10 | 10 | 10 |
| Annual DHW discharge energy [kWh/year] | 3038 | 3038 | 2691 | 2691 |
| Design Supply temperature for SH [°C] | 35 | 55 | 35 | 55 |
| Design Return temperature for SH [°C] | 30 | 45 | 30 | 45 |
| Specific SH heating demand [kWh/(m$^2$ year)] | 59 | 123 | 23 | 62 |
| Annual SH demand [kWh/year] | 8269 | 17224 | 3673 | 9172 |

| | | | | |
|---|---|---|---|---|
| Design SH load [kW] | 4.4 | 7.7 | 3.8 | 6.8 |
| Air source HP capacity @A2W35 [kW] | 8.5 | 14.5 | 8.5 | 14.5 |
| Ground source HP capacity @B0W35 [kW] | 4.9 | 8.2 | 4.9 | 8.2 |
| Borehole depth [m] | 75 | 123 | 75 | 123 |

For this study, the space heat distribution pump was included in the total electricity use. Penalty factors for DHW production ($W_{el,DHW,pen}$) and SH ($W_{el,SH,pen}$) were defined as in [34] and in addition were kept lower than 1% of total DHW energy ($Q_{DHW}$) and of total SH energy ($Q_{SH}$), respectively, for all simulations. Total electricity use ($W_{el,SHP+,pen}$) and seasonal performance factors ($SPF_{SHP+,pen}$), defined in Eq. (1) and (2), were used for the comparison of results.

$$W_{el,SHP+,pen} = W_{el,HP} + W_{el,SC} + W_{el,EH} + W_{el,Ctr} + W_{el,dist} + W_{el,DHW,pen} + W_{el,SH,pen} \quad (1)$$

$$SPF_{SHP+,pen} = (Q_{SH} + Q_{DHW}) / W_{el,SHP+,pen} \quad (2)$$

where $W_{el,HP}$ is the total electrical energy use of the heat pump, $W_{el,SC}$ is the total electrical energy use of solar circuit, $W_{el,EH}$ is the total electrical energy use of auxiliary electrical heater, $W_{el,Ctr}$ is the total electrical energy use of controller, $W_{el,dist}$ is the total electrical energy use of all circulation pumps.

Two reference systems were defined for this study, one with GSHP and one with ASHP, and were based on state of the art of solar thermal combisystems with heat pumps with parallel configuration. The parameter values for the models were derived from measurement data from specific component tests carried out at test institutes or, in the case of the heat pump, from the manufacturer. The heat pumps and boreholes were sized using a simple sizing rule for the Zurich climate and the given building, whereas the store and collector were standard sizes for such solar and heat pump system packages. Details are given in the following chapter. The complete system models were not verified against measured data.

Results for all system variations were compared to those for the reference systems according to Eq. (3) and Eq. (4)

$$\Delta W_{el,SHP+,pen} = W_{el,SHP+,V,pen} - W_{el,SHP+,pen} \quad (3)$$

$$\Delta SPF_{SHP+,pen} = (SPF_{SHP+,V,pen} - SPF_{SHP+,pen}) / SPF_{SHP+,pen} \quad (4)$$

where $W_{el,SHP+,V,pen}$ is the total electrical energy use for the system variation and similarly for $SPF_{SHP+,V,pen}$. A negative value of $\Delta W_{el,SHP+,pen}$ and $\Delta SPF_{SHP+,pen}$ means a reduction in electric energy use and SPF respectively compared to the reference solution.

### 2.1. System Description

A schematic of the reference system with ASHP is shown in Fig.1, which is chosen to be a typical state of the art system. The system with GSHP is exactly the same apart from the borehole heat exchanger, which is connected to the evaporator of the heat pump, and the control of the heat pump compressor, which has fixed speed while the ASHP has variable speed. The system layout is typical for what was available on the market at the time of the study.

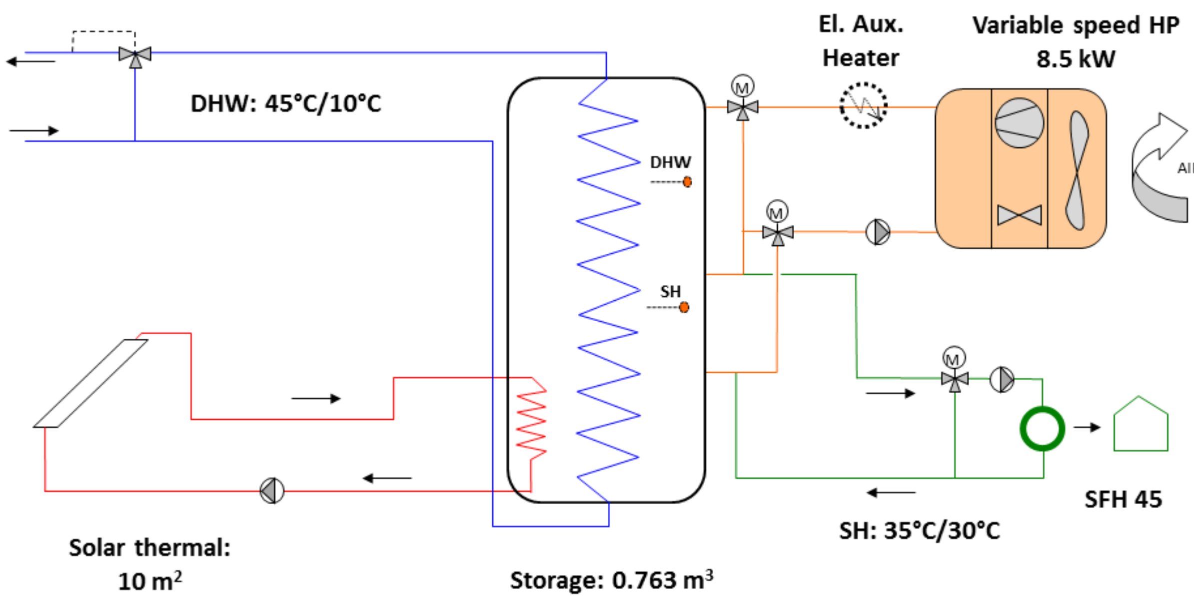


Fig. 1 Schematic of air source reference system. The position of the temperature sensors in the storage tank for space heating preparation (SH) and for hot water charge (DHW) is shown. Details of sensor heights are given in Table 4.

The investigated system is a parallel system with solar collectors that charge the hot water store via an internal heat exchanger and a heat pump that either charges the main store or serves the space heat load directly. Solar thermal consists of flat plate collectors that are tilted 45° and orientated to the south. The total absorber area for four modules is 9.28 $m^2$, which is a typical size for this kind of system. The 750 liters water store has a solar coil in the lower volume and a stainless steel internal coil heat exchanger that covers the whole store height for the preparation of DHW.

The ASHP is a R410A split unit coupled with a variable speed compressor whereas the GSHP is coupled to a borehole heat exchanger and is run at constant compressor speed. In the simulation model a scale factor has been used to size the heat pumps for design conditions that were defined as being the maximum space heating load during the year for a 24 hour period plus an extra 0.5 kW for charging the store for DHW preparation, which is 50% higher than the average DHW load during the year. This sizing is for the volumetric flow rate (compressor size) as well as heat exchanger sizes (UA-values). This results in a heating capacity that is very different for the two heat pumps at standard conditions due to the large difference in evaporation temperatures at design conditions (see Table 1). This sizing approach means that the heat pumps provides virtually all the heat over the year for the Zurich climate, with very little required from the auxiliary electrical heater.  For the Carcassonne climate the heat pump is slightly “oversized” as the design heating load is about 12% lower than in Zurich. The heat pump is connected to the store via three-way valves so that it charges either the upper volume for DHW preparation or the middle volume for space heating, a so called four pipe connection. The space heating loop is connected in parallel to the space heating part of the store. When the store is charged for space heating, part of the flow goes via the space heating distribution system and the rest through the store, depending on the operating conditions. The maximum flow through the heat distribution system is lower than that through the HP and is further decreased by thermostatic valves to maintain the desired room set temperature.

The supply temperature to the heat distribution system is dependent on the outside ambient temperature (heating curve) as is common in central Europe. The design supply temperatures are defined in Table 2 and design outside ambient temperature in Table 1. Different design supply temperatures are chosen as previous research has shown that the system performance of solar combisystems is very dependent on the temperature level of the heating system [4, 23, 27, 28], which is due to the different exergy efficiency of both the heating system and other system components [35]. Two typical design heat supply temperatures are chosen, one for radiators (higher temperature) and one for floor heating (lower temperature).

The heat pump stops and space heat is delivered from the store instead when the temperature in the return line to the heat pump goes above the current supply temperature according to the heating curve. The heat pump is started again in space heating mode when the temperature sensor in the store for heating drops below this same set point temperature minus a hysteresis of 3 K. This temperature sensor is located in between the heat pump inlet and outlet connection of the heating volume of the store (see Fig. 1). For the ASHP with variable speed compressor, the speed is controlled in order to deliver the flow temperature based on the heating curve. In DHW mode the control principle is the same, with the exception that the compressor always runs at full speed (also for the ASHP) during the whole charging process and the temperature sensor is located in the upper part of the store. The set point temperature is chosen according to the required temperature for DHW preparation. A single sensor is used for on/off, with a hysteresis of 4 K.

An auxiliary heater is placed in series with the heat pump before the three-way valve between heat pump and store. The auxiliary heater switches on when the heat pump cannot supply the set point temperature for SH or DHW preparation. It switches off once the temperature of the heat pump supply line reaches the set point temperature.

## 2.2. System Modelling

The model parameters were derived for component products that are available in the market. The component model parameters are all based on experimental results, but the whole system model was not validated against measurements. Table 3 shows how system components were modelled.

Table 3 Details of how the system components were modelled. The parameters of collector, storage tank and heat pump were derived for component products while typical values were used for pumps and pipes and based from state of the art systems.

| ***Component*** | ***TRNSYS Type*** | ***Source for parameters*** |
|---|---|---|
| Collector | 832 | [36] |
| Storage Tank | 340 | [37, 41] |
| Heat Pump | 877 | [38] |
| Circulation Pumps | Equations | Typical values |
| Pipes | 31 | Typical values |

Type 832 QDT [39] multinode was used for modelling the collector field. Type 340 [40], which is a multiport and one dimensional multinode model, was used for modelling the thermal storage and parameters were derived from a test of a state of the art combistore according to EN 12977-3 [41]. Heat pump connections for charging the tank were modelled via two double ports as fixed inlets, one for DHW mode and one for SH mode. Space heating discharge to the heating loop was modelled via a separate double port. The simulation model assumed that the inlets to the store did not disturb the stratification due to the high flow rates that normally exist in systems with heat pumps. The effect of high flow rates on the disturbance of storage stratification for a tank of 795 liters was investigated by Haller et al. in [42] who found that significant de-stratification occurs unless active measures are made to avoid it. The internal heat exchangers for DHW preparation and solar collector charge were modelled as internal spiral heat exchangers. Details of sensor, heat exchanger and double port connection parameters are shown in Table 4 together with parameters for the UA-value of the heat exchangers. The total UA-value for heat losses of 3.78 W/K was split into top, bottom and side losses, which is a relatively high value compared to systems analysed in IEA-SHC Task 26 [28], resulting in heat losses of ~1100 kWh/year in Zurich for the reference system. The vertical thermal conductivity was set to 0.6 W/(m K), the value for water.

Table 4 Sensor and double port connection parameters. All heights are given as relative to the height of the store, with zero being at the bottom. For the heat exchangers, the UA-value for the heat transfer is calculated as $\boldsymbol{UA = UA_0 \cdot \dot{m}^{b_0} \cdot T_m^{b_1}}$, where $\boldsymbol{\dot{m}}$ is the mass flow in the heat exchanger in kg/s and $T_m$ [°C] is the average of the inlet temperature to the heat exchanger and the store temperature at that level in the store [40].

| ***Parameter*** | ***Heat pump DHW charge*** | ***Heat pump SH charge*** | ***SH discharge*** | ***Solar charge*** | ***DHW discharge*** |
|---|---|---|---|---|---|
| Inlet height [-] | 1.0 | 0.49 | 0.26 | 0.45 | 0.03 |
| Outlet height [-] | 0.49 | 0.26 | 0.49 | 0.00 | 0.95 |
| Sensor height [-] | 0.65 | 0.44 | - | 0.18 | - |
| Heat exchanger[1]<br>Volume [liters]<br>Base UA-value, $UA_0$ [W/K)]<br>Mass flow exponent, $b_0$ [-]<br>Temperature exponent, $b_1$ [-] | - | - | - | <br>12<br>312<br>0.39<br>0.42 | <br>33<br>368<br>0.39<br>0.86 |

The heat pump was modelled by using Type 877 [43]. Type 877 is a semi-physical model for compression heat pumps based on a calculation of the thermodynamic refrigerant cycle and the thermal properties of the used refrigerant. The thermodynamic properties of the working fluid are obtained by polynomial curve fits, which have been determined separately for the two-phase and the superheated domain of the different refrigerants. A performance map of the compressor, or alternatively an approach based on overall isentropic and volumetric efficiency, is used for the simulation of the compressor efficiency and the electricity consumption. Compressor heat losses to the ambient can be modelled either as a percentage of the compressor electrical power or with a UA-value for the heat losses from the compressor to the ambient. Start and stop losses (start/stop) of the heat pump are considered by using a time constant, depending on the time the heat pump has been switched on and time period since it was last switched off. Start/stop losses are subtracted from the condenser heating capacity, thus reducing the efficiency of the cycle. The losses caused by the icing of the air source evaporator and its defrosting are considered in a very simple way. The amount of ice that is expected to be built under the operating conditions is calculated depending on the evaporation temperature and the temperature, relative humidity and pressure of the air at inlet/outlet of the heat exchanger. The heating capacity needed for the melting of the ice is calculated using an additional defrosting efficiency parameter and then subtracted from the condenser heating capacity, thus reducing the efficiency of the cycle. The dynamics of the defrosting are not considered by the model, instead a value of 0.5 for the defrost efficiency was assumed. Every heat exchanger in the cycle is calculated using the inlet conditions ($\dot{m}$, p, T) of the fluids on both sides and the

UA-value (W/K) of the respective heat exchanger. The model includes the possibility to use air, brine or both as a heat source (dual source evaporators) and the possibility to use an extra desuperheater heat exchanger in addition to the condenser, e.g. for DHW preparation.

In this study the heat pump was modelled by using the approach based on overall isentropic and volumetric efficiency. Compressor heat losses were modelled as with a percentage of the electrical power of the compressor. In the case of ASHP, the percentage value varied according to the compressor speed and the pressure ratio, while in the case of GSHP a fixed value for all conditions was assumed. Model parameters were chosen in order to fit the heat pump for which detailed test data were available from the manufacturer. A scale factor approach was used to size the heat pump so that it could supply 100% of the design heating load for the climate of Zurich and for each of the two buildings. The scale factor was used for the UA-values of heat exchangers, the swept volume flow rate of heat pump compressor, mass flow of condenser (water side) and evaporator (air or brine side) while the overall isentropic and volumetric efficiencies of the compressor were kept the same.

Pipes connecting the collector to the store and between store and heat pump were modelled explicitly using Type 31. The dimension of the pipes in the collector circuit was defined according to prEN 12977-2:2007 [44] depending on the flow rate, as was the insulation standard. The insulation standard of the other pipes was defined using the same standard, but the pipe diameter was chosen according to thumb rules used by plumbers. Pipe runs were estimated for a standard installation resulting in 30 m piping in the collector loop (internal diameter 16 mm) and a total of 22 m for all the other pipes (internal diameter 25 mm). The heat loss UA-value for the pipes was calculated theoretically based on the insulation level but adjusted for heat losses from connections and pipes. 0.085 W/K (equivalent to a bare copper pipe of 0.1 m with diameter 0.035 m) was added for each connection and 0.17 W/K for each component such as a valve (equivalent to a bare copper pipe of 0.2 m with diameter 0.035 m). In total 18 connections and 10 components were included.

The electricity use of the pumps was not derived from the component models but was calculated separately in a set of equations using a nominal power for set conditions of pressure drop and flow rate. Corrections were applied depending on the actual flow rate and the (linear) dependency of the efficiency on the flow rate. Nominal efficiencies of 12% for the solar loop pump and 40% for the pumps used for charging the store from the heat pump were used. A fixed power of 15 W was used for the high efficiency SH distribution pump.

### 2.3. Parametric studies

A systematic series of parametric studies was carried out to show the impact of climate, load and heat source for the heat pump. The impact of component size was studied by using scale factors (0.50, 0.75, 1.50) for the size of collector area, the tank volume, the annual DHW discharge energy, the UA-value of DHW heat exchanger and the heat pump size.

All system variations provided the same comfort requirements for the indoor temperature and DHW supply temperature. In cases when the system did not provide the desired level of comfort for DHW preparation with the base case values, the set temperature for DHW charge was increased so that more heat was stored in the DHW volume of the tank.

## 3. Results and Discussion

### 3.1. Reference Systems

Table 5 shows results for the two reference systems for the range of two climates and buildings.

Table 5 SPF and total electricity use for the two reference systems for the two climates and buildings.

| | ***AZ45*** | ***GZ45*** | ***AZ100*** | ***GZ100*** | ***AC45*** | ***GC45*** | ***AC100*** | ***GC100*** |
|---|---|---|---|---|---|---|---|---|
| $SPF_{SHP+,pen}$ [-] | 3.16 | 4.12 | 2.43 | 3.45 | 3.85 | 5.80 | 2.93 | 4.58 |
| $W_{el,SHP+,pen}$ [kWh/year] | 3581 | 2668 | 8340 | 5773 | 1655 | 1035 | 4055 | 2488 |

The total electricity use varies from 1035 to 8340 kWh/year while the system SPF varies from 5.80 to 2.43 in reverse order. This gives a factor of over five in electricity use from the largest to the smallest values, giving a wide range of conditions for the systems. The SPF values for Carcassonne are better than those shown for similar system in IEA SHC Task 44 / HPP Annex 38 [30] for Strasbourg while those of Zurich are slightly lower. This is true for both the SFH45 and SFH100 buildings that are the same in both studies. This is consistent with the difference in climate conditions of Strasbourg that has an average ambient temperature that is between that of Carcassonne and Zurich. Fig. 2 shows the overall system thermal values for the two reference systems. There is a significant difference between the total heat energies in and out from the systems. This is because the ASHP system has much greater auxiliary losses than the GSHP system. Auxiliary losses include the start/stop losses of heat pump cycle, the compressor heat losses to ambient and losses due to defrosting.

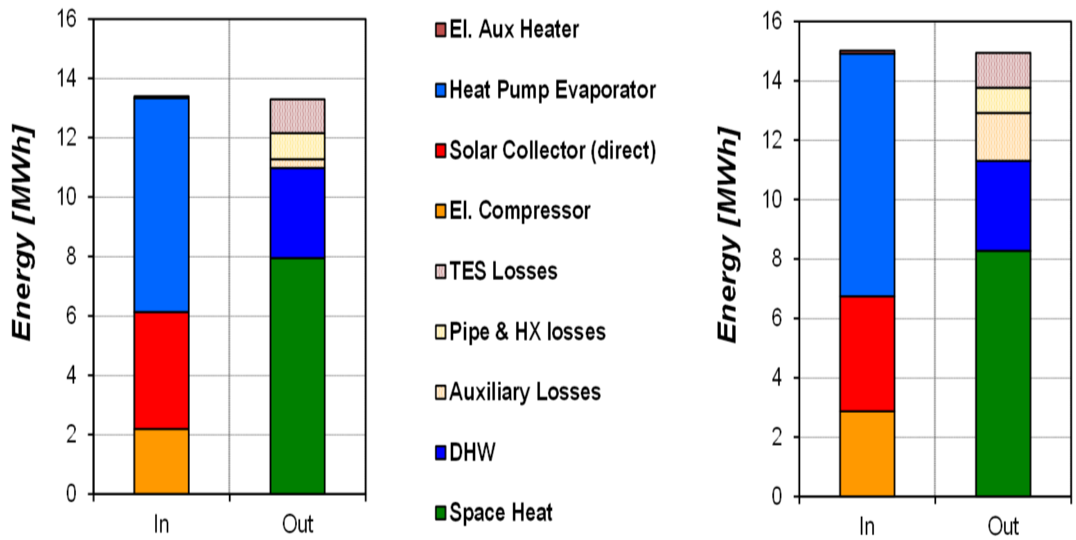


Fig. 2 Overall system results for the two reference systems (only thermally active parts). GSHP (left) and ASHP (right).

Fig. 3 shows the energy balance of the stores in the two reference systems. Again, there is a significant difference between the behaviour of the two systems, with the GSHP using the store a lot more for the space heating compared to the ASHP. This is due to the fact that the ASHP has a variable speed compressor, which means that there are fewer times when the store is charged and then discharged.

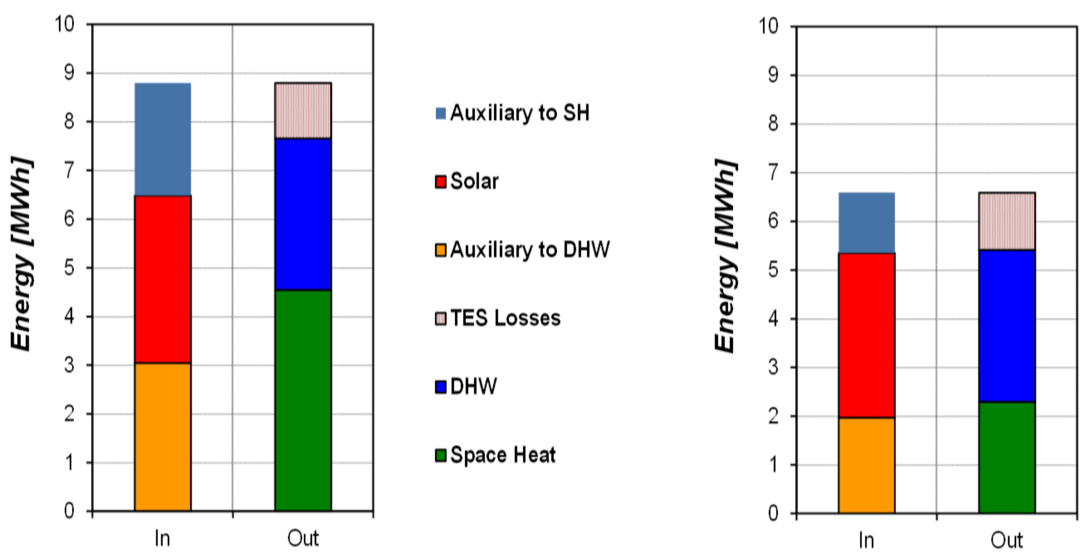


Fig. 3 Heat input and output from the stores in the two reference systems. GSHP (left) and ASHP (right).

Fig. 4 shows heat balance for the heat pump in the two systems. The much greater compressor heat losses to the ambient in the case of ASHP (>900 kWh/year) are mainly responsible for the larger variation of energy use of ASHP. The reason is that the ASHP is a split-system, which is normally employed in air-conditioning and therefore, the compressor is not optimized for heating purposes. Heat pump losses due to the defrosting of the outdoor evaporator heat exchanger also contribute to a larger energy use in the case of ASHP and in the amount of 318 kWh/year. ASHP supplies a much larger part of the space heating load directly to the space heating loop, while GSHP has a larger amount of heat supplied to the DHW part of the store.

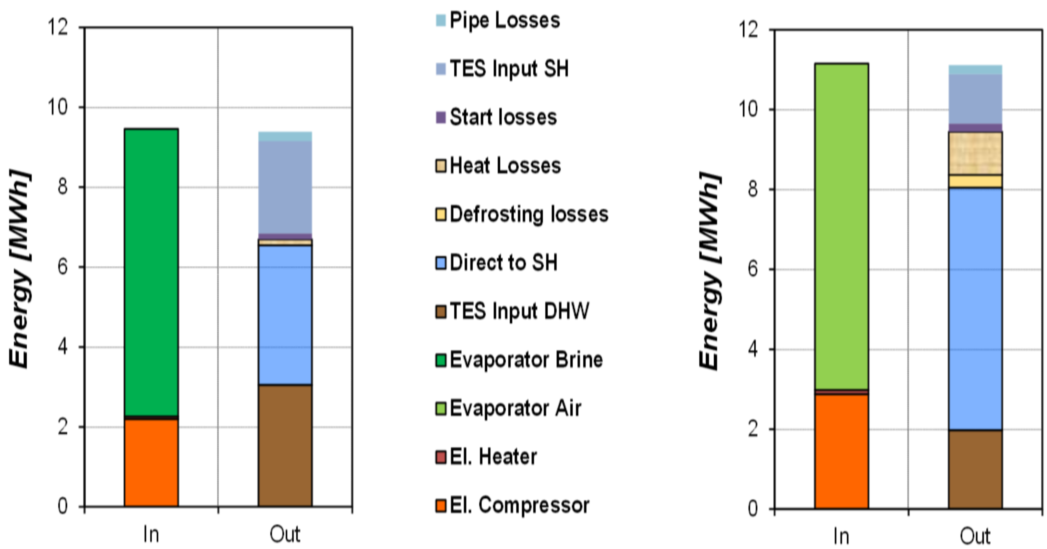


Fig. 4 Heat balance for heat pump in the two reference systems. GSHP (left) and ASHP (right).

Fig. 5 shows the electricity use in the two reference systems. The use of the electrical auxiliary heater is relatively small in both systems with a slightly larger share in the case of ASHP. Over 80% is used by the compressor, whereas pumps only use 8% and 4% in the GSHP and ASHP systems respectively. The fan in the ASHP uses 8% while the parasitic energy consumption of controllers and electric devices has a share of 7% and 5% respectively in the GSHP and ASHP systems respectively.

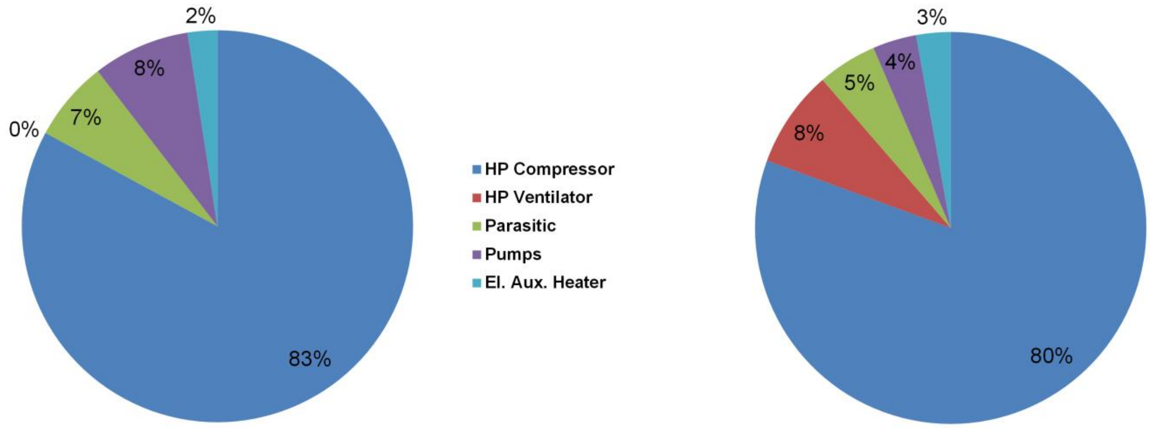


Fig. 5 Electricity use in the two reference systems. GSHP (left) and ASHP (right).

## 3.2. Parametric studies

In the following parametric studies results for the matrix of heat pump heat source, building as well as climate are shown in all figures.

### 3.2.1. Annual DHW discharge energy

DHW discharge energy varies from 1519 kWh/year (scale factor 0.50) to 4557 kWh/year (scale factor 1.50) for Zurich and similarly from 1346 kWh/year to 4037 kWh/year for Carcassonne. Total tank volume was kept the same as in the reference for the whole range, as well as the proportion between tank volume and DHW volume. Fig. 6 shows the change in $\Delta W_{el,SHP+,pen}$ as a function of the annual DHW discharge energy. The changes for Carcassonne are much smaller than for Zurich, and changes are also smaller for GSHP than for ASHP. This can be explained by the fact that the change in $Q_{DHW}$ is lower while the change in solar gain is larger in Carcassonne compared to Zurich. A superior SPF explains why the change is smaller for the GSHP than for the ASHP. The difference between SFH45 and SFH100 for a given climate and heat pump is small, which is to be expected as it is the DHW load that has changed and not the SH load. An exception to the above is for GZ45, where the set temperature for the DHW volume of the store had to be increased from 52°C to 58°C for scale factor 1.50.

There are several reasons why just this case is different. For a given set temperature it was found that the store temperature varied between the different cases, with GZ45 having lowest temperatures. Results show that the average temperature of the upper 10% of the store is 49°C for GZ45 while it is over 51°C for AZ45. ASHP has an increase in heating capacity as the evaporator temperature increases, i.e. when air temperature increases, and this leads to an increase in compressor discharge temperature. For the SFH100 house, the heating system works at higher operating temperature and thus, the average temperature of the store is higher than in the SFH45 house. In Carcassonne the larger solar gain is the reason for the higher store temperature compared to Zurich.

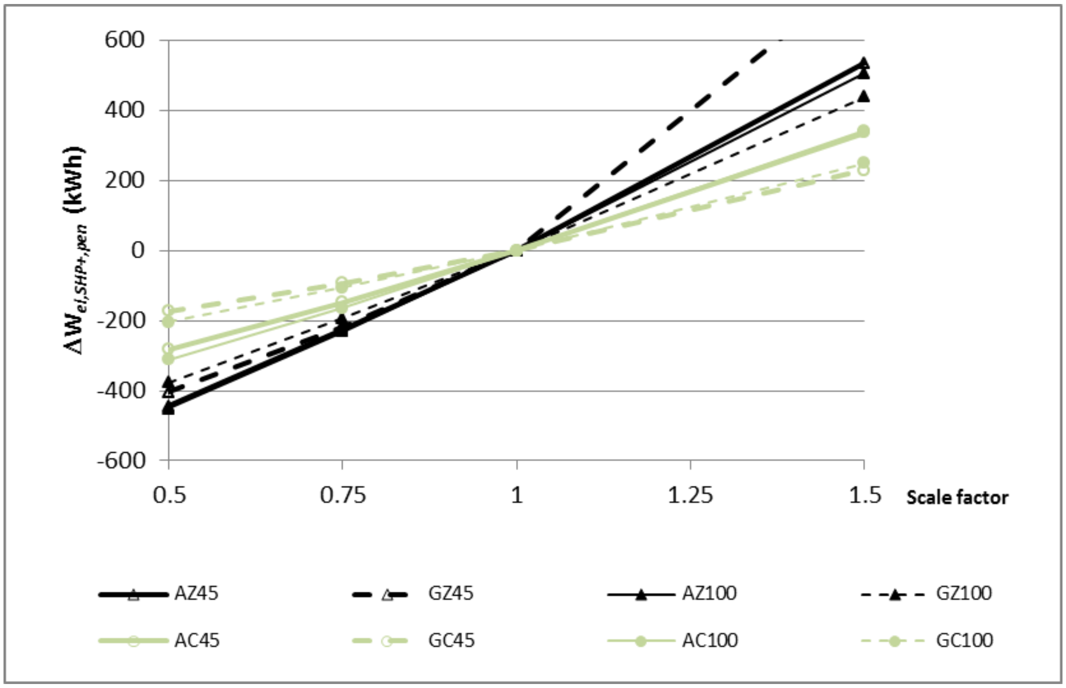


Fig. 6 Change in system electricity use as function of the DHW discharge energy.

### 3.2.2.Collector area

Fig. 7 shows the change in $\Delta W_{el,SHP+,pen}$ as a function of the size of the collector. The range is from 4.64 $m^2$ (scale factor 0.50) to 13.92 $m^2$ (scale factor 1.50). The specific storage volume is also given in (litres per $m^2$ collector area). $\Delta W_{el,SHP+,pen}$ is larger for ASHP than GSHP and for high energy buildings, however the differences are relatively small.  As expected, $\Delta W_{el,SHP+,pen}$ is smaller for larger collector areas thanks to the larger amount of solar heat available in the tank that reduces the use of heat pump, with the biggest variation being for the ASHP and for the SFH100 building. There are very small differences in results between the climates of Carcassonne and Zurich for the ASHP, whereas there are larger differences for the GSHP. Tank heat losses increase, but they have a very small impact on system results. These results are consistent with those found by IEA SHC Task 44 / HPP Annex 38 [30], both in terms of greater changes for ASHP than GSHP but also in terms of increased electricity savings for increased collector area.

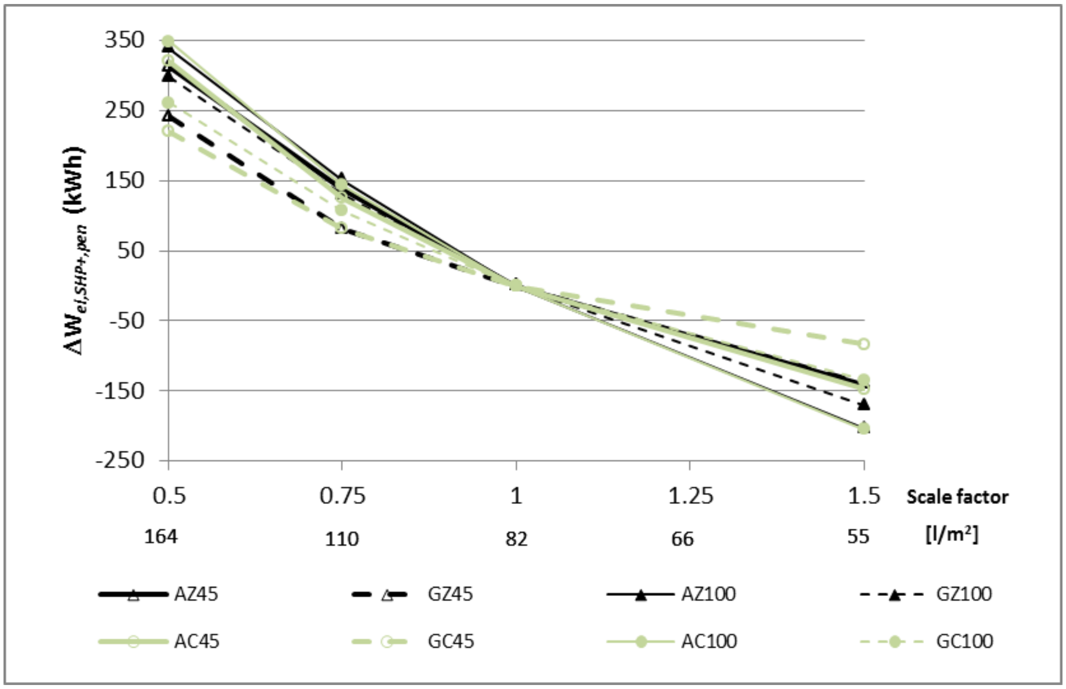


Fig. 7 Change in system electricity use as function of the size of the collector.

The FSC for the combination of two climates and two house standards and for different collector areas ranged from 0.22 (scale factor 0.50 and largest load) to 0.91 (scale factor 1.50 and smallest load).

### 3.2.3. Tank volume

Fig. 8 shows the change in $\Delta W_{el,SHP+,pen}$ as a function of the tank volume. The range is from 0.38 $m^3$ (scale factor 0.50) to 1.13 $m^3$ (scale factor 1.50). The specific storage volume is also given. The proportion of the volume devoted to DHW was kept the same, which means that the DHW volume was also varied from 0.19 $m^3$ to 0.57 $m^3$. As with collector size, the change in electricity use is greater for the SFH100 building than for the SFH45 and for the ASHP compared to the GSHP. For scale factors between 0.50 and 1.00 $\Delta W_{el,SHP+,pen}$ for Zurich is larger than for Carcassonne and vice versa between 1.00 and 1.50. $\Delta W_{el,SHP+,pen}$ is smaller for bigger tank volume and for ASHP rather than GSHP, but differences are small. The values for GZ45 at scale factors 0.75 and 0.50 are higher because the DHW charge set temperature had to be increased to 55°C and 58°C respectively in order to keep DHW penalties below 1%. In all other cases the default value of 52°C could be kept. The reasons for the different DHW temperature settings for GZ45 are the same of those for the study on the annual DHW discharge. Due to the higher settings for the DHW charge set temperature, the increase of electricity use at scale factors 0.50 and 0.75 for GZ45 is roughly 2.5 times higher than the average of all combinations of building/climate.

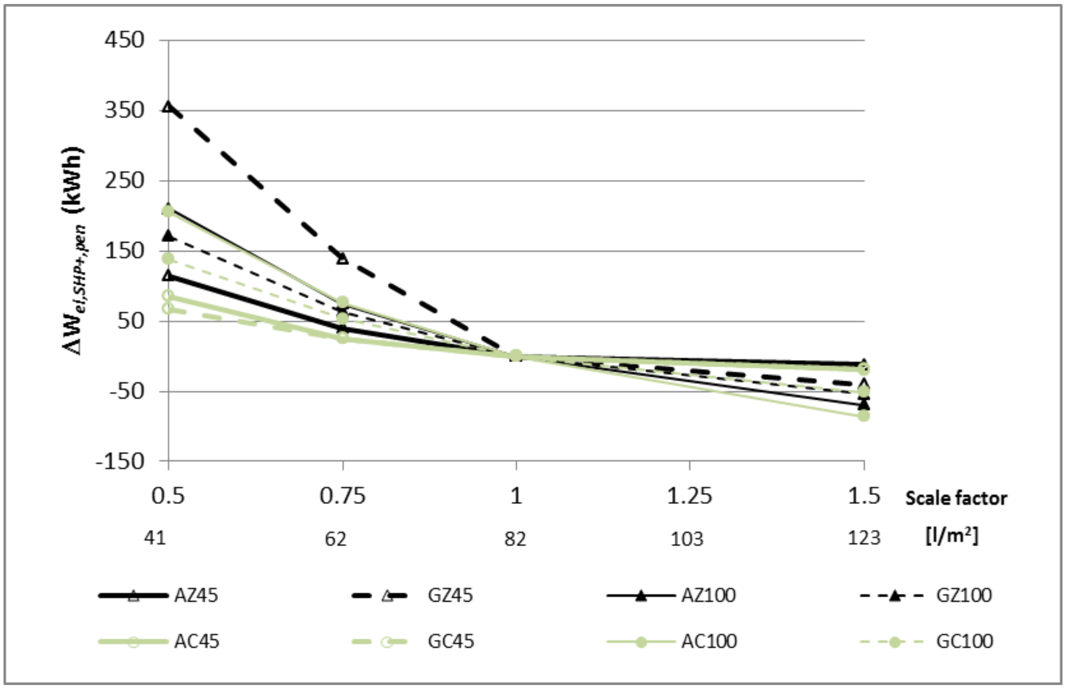


Fig. 8 Change in system electricity use as function of the size of the tank volume.

### 3.2.4.UA-value of DHW heat exchanger

Fig. 9 shows the change in $\Delta W_{el,SHP+,pen}$ as a function of the UA-value of DHW heat exchanger. The range is from 184 W/K (scale factor 0.50) to 552 W/K (scale factor 1.50) for the base UA-value (see table 2). Settings of DHW charge were adapted in each case so that the penalties were kept below 1%. This resulted in set temperatures of 55°C, 52°C, 50°C and 47°C respectively for 0.50, 0.75, 1.00 and 1.50 for all combinations of climate/building except for GZ45, where settings of 59°C, 57°C, 55°C and 53°C respectively were required. The reason for the different settings for GZ45 was already explained above.

As expected, $\Delta W_{el,SHP+,pen}$ is smaller at larger scale factors thanks to a larger amount of heat transferred to the top of the tank. $\Delta W_{el,SHP+,pen}$ is larger for ASHP than for GSHP, for Zurich compared to Carcassonne and for SFH100 compared to SFH45. The whole range varies between -138 kWh/year and 303 kWh/year of change in total electrical consumption compared to the reference, which is similar to the range shown for both the collector area and storage volume. Thus the combination of DHW heat exchanger size and the optimised charge temperature for the DHW volume has a significant impact on results. The impact on energy savings is larger in this study than those found in IEA-SHC Task 26 [28]. This is due to the fact that in this study the set temperature is changed to just meet the DHW load with penalties less than 1%. This decrease in set temperature leads to the majority of the savings, and the savings due to a given reduction in set temperature is larger for systems with heat pumps than it is for those in [28] that use gas or electricity as an auxiliary.

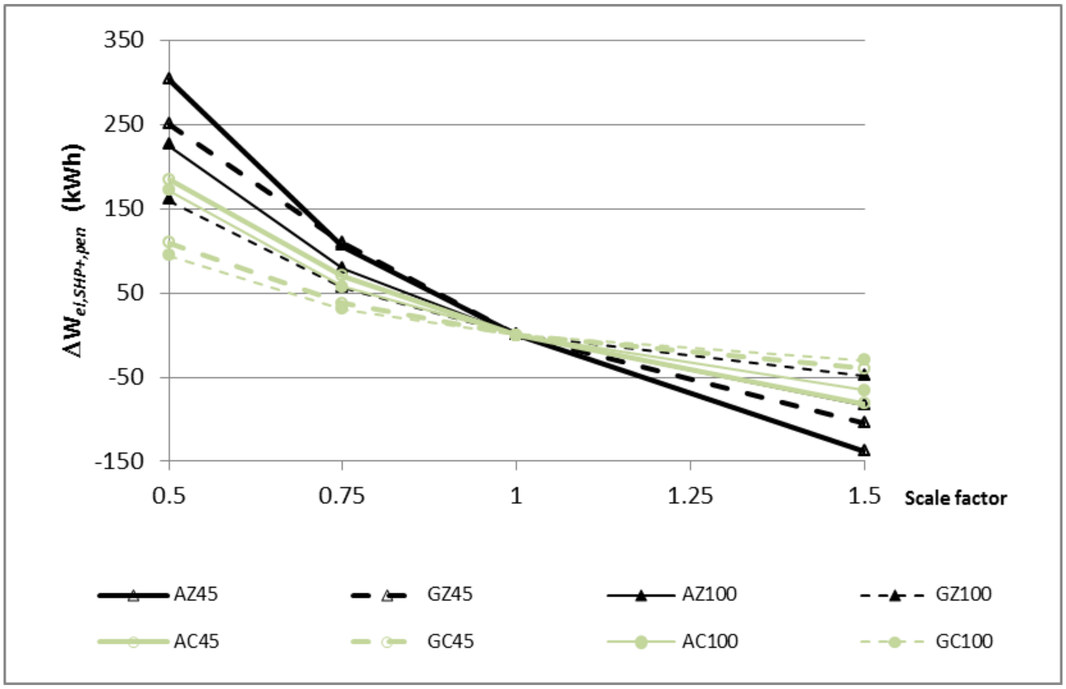


Fig. 9 Change in system electricity use as function of UA-value of DHW heat exchanger.

### 3.2.5. Size of Heat pump

Fig. 10 shows the change in $\Delta W_{el,SHP+,pen}$ as a function of the size of heat pump. The range is only for scale factor from 0.75 to 1.50 as most sizing rules suggest values of at least 75% of the design heating load. For a scale factor 0.5, the increase of the auxiliary electrical heater use is significant, especially in the climate of Zurich, where for the GSHP the electrical heater ($W_{el,EH}$) uses over 40% of the total system electricity use, which confirms the suitability of not sizing the heat pump too small. For the Carcassonne climate the use of electrical heater is smaller (Table 6), partly due to the fact that the heat pump was already "oversized" by 12% due to the sizing criteria used in the study. Fig. 10 shows that there are both reductions and increases in system electricity use when the size of the heat pump is increased and decreased, and that the results depend on the climate, heat pump type and load. Variations are largest for the Zurich climate, with variations for Carcassonne being relatively small. This is partly due to the fact that the total electricity use is smaller in Carcassonne than in Zurich. There are two main influences on these results: the heat pump start/stop losses and the use of auxiliary electrical heater.

Table6 Electricity use of the auxiliary electrical heater ($W_{el,EH,1.0}$) and total heat pump losses ($Q_{LOSS,1.0}$) for scale factor 1.0. The ratio of compressor heat losses ($Q_{LOSS,cpr}$ / $Q_{,LOSS}$) to the total heat pump losses and the share of heat pump start/stop losses ($Q_{LOSS,Start/stop}$ / $Q_{,LOSS}$) to the total heat pump losses are given for scale factor 0.75 and 1.5.

| | ***AZ45*** | | ***GZ45*** | | ***AZ100*** | | ***GZ100*** | | ***AC45*** | | ***GC45*** | | ***AC100*** | | ***GC100*** | |
|---|---|---|---|---|---|---|---|---|---|---|---|---|---|---|---|---|
| $W_{el,EH,1.0}$ [kWh/year] | 137 | | 176 | | 272 | | 521 | | 36 | | 11 | | 86 | | 61 | |
| $Q_{HP,LOSS,1.0}$ [kWh/year] | 1540 | | 290 | | 4165 | | 790 | | 777 | | 162 | | 2243 | | 535 | |
| $Q_{LOSS,cpr}$ / $Q_{HP,LOSS}$ [%] | 70 (0.75) | 58 (1.5) | 62 (0.75) | 32 (1.5) | 80 (0.75) | 64 (1.5) | 58 (0.75) | 30 (1.5) | 59 (0.75) | 44 (1.5) | 41 (0.75) | 20 (1.5) | 68 (0.75) | 45 (1.5) | 35 (0.75) | 19 (1.5) |
| $Q_{LOSS,Start/stop}$ / $Q_{HP,LOSS}$ [%] | 7 (0.75) | 26 (1.5) | 38 (0.75) | 68 (1.5) | 8 (0.75) | 27 (1.5) | 42 (0.75) | 70 (1.5) | 15 (0.75) | 35 (1.5) | 59 (0.75) | 80 (1.5) | 19 (0.75) | 44 (1.5) | 65 (0.75) | 81 (1.5) |

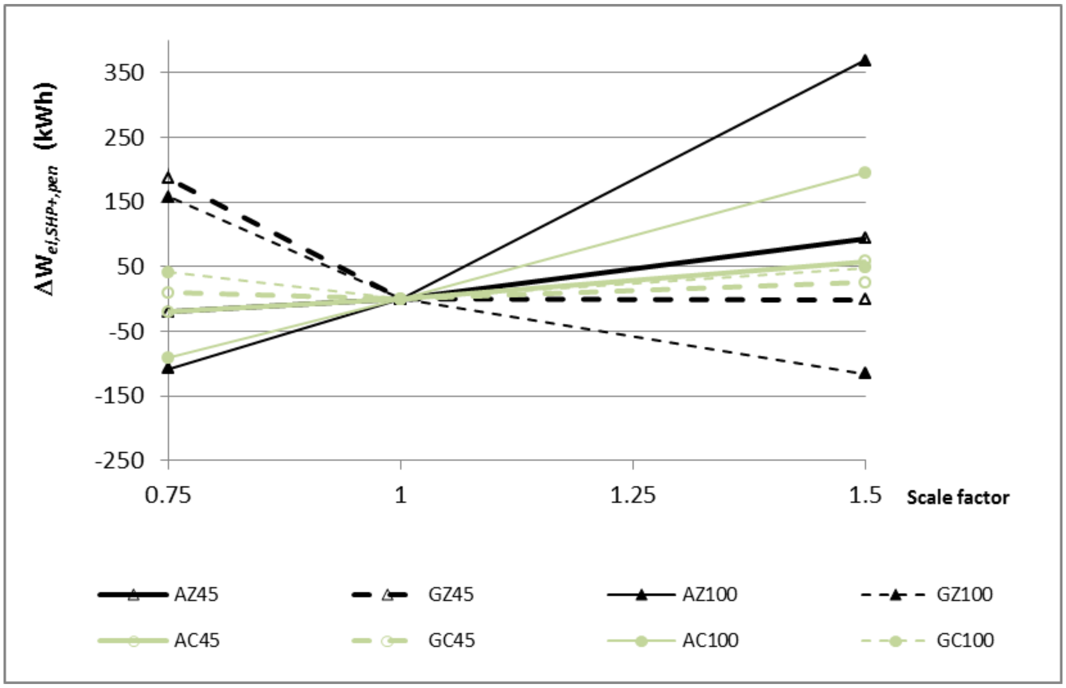


Fig. 10 Change in system electricity use as function of the size of heat pump.

Fig.11 shows the change in start/stop losses as a function of the size of heat pump. These losses increase with increasing in heat pump size and with larger change for ASHP in the SFH100 due to the larger use of heat pump. However, the impact of start/stop losses on total heat pump losses is bigger for GSHP than for ASHP as shown in Table 6. For a scale factor 1.50, start/stop losses cover the 70% of total heat pump losses in the SFH100 in Zurich and 81% in Carcassonne. Larger percentage for Carcassonne is justified by the large number of compressor starts and stops that occur because the heat pump is oversized. Table 6 shows also that the ratio of compressor heat losses to the total heat pump losses is smaller for GSHP than for ASHP, thus the reason for the bigger start/stop losses. Compressor heat losses to the ambient increase with decreasing in heat pump size since smaller heat pumps run at full speed for longer periods. However, the change as a function of the size of heat pump is not nearly as significant as the change in start/stop losses.

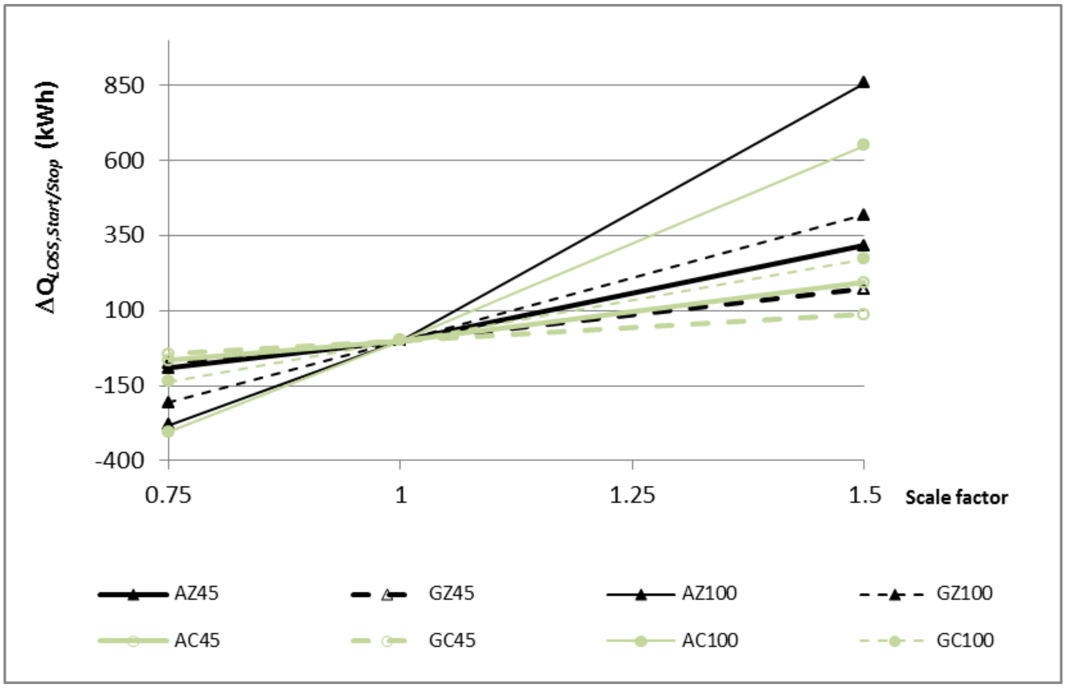


Fig. 11 Change in heat pump start/stop losses as function of the size of heat pump.

Fig. 12 shows the use of the auxiliary electrical heater as a function of the size of heat pump. This varies in the opposite way to the heat losses, with decreasing auxiliary electricity use with increasing scale factor. There is a greater variation for the GSHP than ASHP as well as SFH100 than SFH45, but the difference between buildings is relatively small. Again the variation for Carcassonne is smaller than for Zurich due to the smaller absolute demand there. For GSHP and SFH45 in Zurich the change between scale 0.75 and 1.0 is much larger than between scale 1.0 and 1.50, whereas for all other cases it is nearly the same.

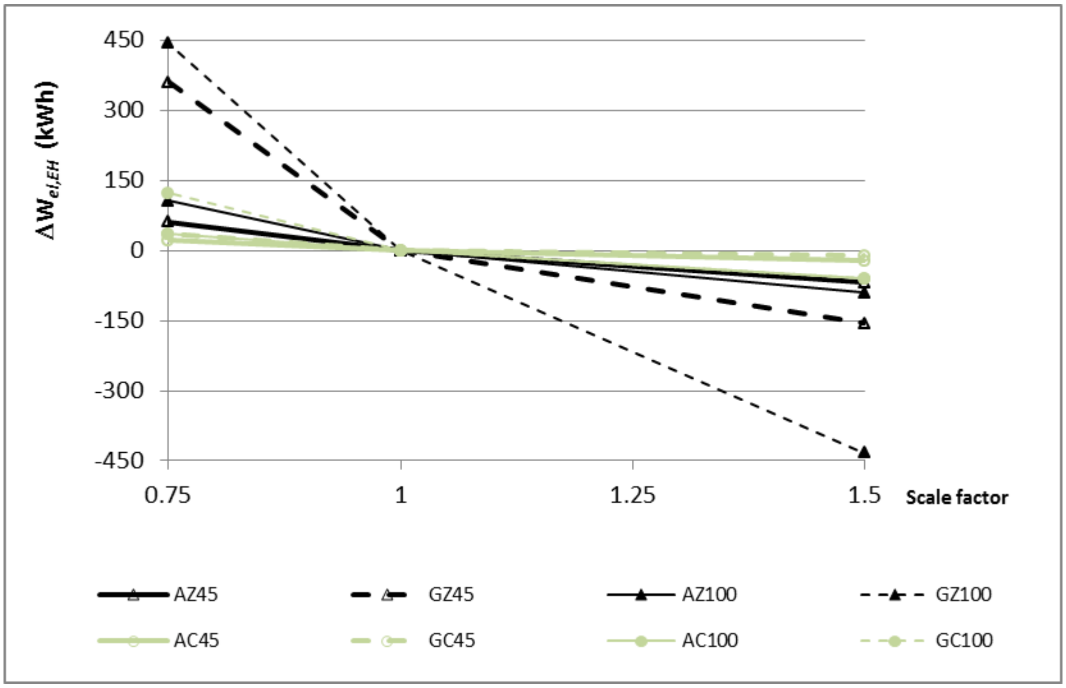


Fig 12 Change in the use of auxiliary electrical heater as function of the size of heat pump.

In combination, these two factors lead to the results in Fig. 10. Start/stop losses and compressor heat losses lead to a larger system electricity use at scale factor 1.50 for the ASHP in the SFH100. Only for the GSHP and for SFH100 in Zurich the system electricity use decreases significantly for scale factor 1.50 and this due to a large reduction in the use of the auxiliary heater. Auxiliary heater is mainly responsible for the larger system electricity use at scale factor 0.75 for the GSHP in the climate of Zurich. This is due the fact that the heat pump heating capacity is insufficient to cover the load for a long period of the heating season. For ASHP, the period when the heat pump capacity is too low is shorter as the capacity increases with decreasing load due to the higher evaporator temperature. For the Carcassonne climate the change was very small, again due to the fact that the heat pump was slightly “oversized”. Interesting results are shown at scale factor 0.75 for ASHP in the SFH100 in both Zurich and Carcassonne, where the reduction of start and stop losses is larger than the increase in the use of auxiliary electrical heater and thus, lead to a reduction in system electricity use.

## 4. Conclusions

The present study focused on the influence of boundary conditions and component size on electricity demand in solar thermal and heat pump combisystems. Two systems were defined and modelled based on state of the art commercial systems for which detailed measurement data were used to derive parameters for the models: one with an air source heat pump (ASHP) and one with a ground source heat pump (GSHP). A combination of two climates, Zurich and Carcassonne, and two houses with different insulation standards (SFH45 and SFH100) was used for the parametric studies in order to give a wide range of boundary conditions.

Simulation results for the system with ASHP for the SFH45 house in Zurich showed a $W_{el,SHP+,pen}$ of 3581 kWh/year and a $SPF_{SHP+,pen}$ of 3.16. The alternative solution with a GSHP showed 25.4% reduction in total electrical use compared to the ASHP system due mainly to the better $SPF_{HP}$ of the GSHP than the ASHP. Moreover, compressor heat losses to the ambient were much higher (>900 kWh/year) for ASHP than for GSHP. In both cases, the heat pump was sized to cover the whole design load, and the annual simulation results showed that only 2-3% of the electricity used was needed by the auxiliary electrical heater for cases where the heat pump could provide for the full load. Pumps, controller and ventilator (only ASHP) accounted for 15-17% of the system electricity use. For the range of climates and loads simulated, $W_{el,SHP,+dist,pen}$ varies from 1035/1655 kWh/year (SFH45 in Carcassonne) to 5773/8340 kWh/year (SFH100 in Zurich) for the GSHP/ASHP reference systems while $SPF_{SHP+,pen}$ varies from 3.85/5.80 to 2.43/3.45 respectively for the same boundary conditions. Changes in DHW demand (volume discharge) were shown to affect electricity use less in Carcassonne than Zurich due to smaller values for energy discharge (high cold water temperature) and higher solar gains.

A sensitivity analysis was also carried out to show the impact of component size on the overall system performance for collector area, tank volume, UA-value of DHW heat exchanger and size of heat pump. Scale factors of 0.50 up to 1.50 of the base case values were used. This was performed for all combinations of climates and buildings as well as for both ASHP and GSHP. Penalties functions were used to ensure that all system variations provided the annual loads for SH and DHW and same level of thermal comfort.

Main conclusions from parametric studies were:

- Larger amount of annual DHW discharge energy had bigger influence on the electricity use for Zurich and for ASHP. This was due to the fact that the change in $Q_{DHW}$ was lower while the change in solar gain was larger in Carcassonne than in Zurich. A superior $SPF_{,HP}$ was the reason for the smaller change for the GSHP than for the ASHP.

- Store temperature varied between the different cases, with the GSHP system in the SFH45 house in Zurich having the lowest temperature of the upper 10% of the hot tank. In order to store more heat in the DHW volume of the tank, the set temperature settings for DHW charge was increased and this caused a large increase in energy use. An alternative solution would be to adjust the height of sensor for the given DHW load.

- Increasing the collector area from 5 to 15 $m^2$ resulted in a decrease between 305 and 552 kWh/year, the smaller values being for the SFH45 building with GSHP while the largest values were for the SFH100 building with ASHP. The fractional solar consumption (FSC), which is the ratio of the usable irradiation available on the collector field to the useful heat delivered, ranged from to 0.22 to 0.91, which is the vast majority of the possible range from 0 to 1. Changing the tank volume had little influence on the electricity use unless the set temperature for the DHW volume in the store had to be increased.
- Changes in the size of the DHW heat exchanger influenced the electricity use more than the store size due to the fact that the DHW set temperature had to be varied with the size to maintain the same comfort level. The range of set temperatures was from 55 °C (scale factor 0.5) to 47 °C (scale factor 1.5). The influence was nearly as large as that of the collector size. The influence was larger for the Zurich climate and for the SFH45 building.
- The influence of the heat pump size was shown to be relatively large, but resulted in both increased and decreased electricity use when decreasing the size of the heat pump by 25% from the base case that covers 100% of design load. The influence was shown to depend on the heat pump start/stop losses and the amount of electricity used by the auxiliary electrical heater.
- Heat pump start/stop losses increased if the size of heat pump increased and had larger relative impact in total heat pump losses for GSHP than for ASHP. These losses influenced the change in electricity use significantly and highlighted the need for a relatively detailed heat pump model when studying system aspects of heat pump systems. The model used in this study was a semi-physical model using refrigerant properties and isentropic and volumetric efficiency of the compressor as well as specific parameters for the various heat loss mechanisms.

## Acknowledgements

The research leading to these results has received funding from the European Union’s Seventh Framework Program FP7/2007-2011 under grant agreement nº 282825 – Acronym MacSheep.

## References

[1] Ruschenburg, J., Herkel, S., Henning, H-M. *A statistical analysis on market-available solar thermal heat pump systems*. Solar Energy. 2013; 95:79-89.

[2] Frank, E., Haller, M., Herkel, S., Ruschenburg, J. *Systematic Classification of Combined Solar Thermal and Heat Pump Systems*. Proc. of the EuroSun 2010 Conference, Graz, Austria.

[3] Haller, M.Y., Frank, E. *On the Potential of Using Heat from Solar Thermal Collectors for Heat Pump Evaporators*. ISES Solar World Congress 2011, Kassel, Germany.

[4] Haller, M.Y., Carbonell, D., Bertram, E., Heinz, A., Bales, C. , Ochs, F. *System Simulations*. In: Hadorn, J. C, editor. Solar and Heat Pump Systems for Residential Buildings. Wiley; in press.

[5] Carbonell, D., Haller, M.Y., Philippen, D., Frank, E. *Simulations of Combined Solar Thermal and Heat Pump Systems for Domestic Hot Water and Space Heating*. Energy Procedia. 2014; 48:524-534.

[6] Haller, M.Y., Haberl, R., Carbonell, D., Philippen, D., Frank, E. *SOL-HEAP - Solar and Heat Pump Combisystems* - Final report, Swiss Federal Office of Energy, 2014.

[7] Colclough, S., McGrath, T. *Net energy analysis of a solar combisystem with Seasonal Thermal Energy Store*. Applied Energy. 2015;147:611-6.

[8] Schimpf, S., Span, R. *Simulation of a solar assisted combined heat pump – Organic rankine cycle system*. Energy Conversion and Management. Available online 25 February 2015.

[9] Asaee, S.R., Ugursal, V.I., Beausoleil-Morrison, I., Ben-Abdallah, N. *Preliminary study for solar combisystem potential in Canadian houses*. Applied Energy. 2014;130:510-8.

[10] Bertram, E., 2013. *Solar assisted heat pump systems with ground heat exchanger – Simulation studies*. Energy Procedia. 2014; 48: 505-514.

[11] Carbonell, D., Haller, M.Y., Frank, E. *Potential benefit of combining heat pumps with solar thermal for heating and domestic hot water preparation*. Energy Procedia. 2014; 57: 2656-2665.

[12] Kaçan, E., Koray, U. *Energy and exergy analysis of solar combisystems*. International Journal of Exergy, 2014; 14(3): 364-387.

[13] Li, H., Sun, L., Zhang, Y. *Performance investigation of a combined solar thermal heat pump heating system*. Applied Thermal Engineering. 2014;71:460-8.

[14] Deng, S., Dai, Y.J., Wang, R.Z. *Performance optimization and analysis of solar combi-system with carbon dioxide heat pump*. Solar Energy. 2013;98:212-25.

[15] Bertram, E., Pärisch, P., Tepe, R. *Impact of solar heat pump system concepts on seasonal performance-Simulation studies*. Proc. of the EuroSun 2012, Rijeka; Opatija, Croatia.

[16] Dott, R., Genkinger, A., Afjei,T. *System Evaluation of Combined Solar & Heat Pump Systems*. Energy Procedia. 2012; 30: 562-570.

[17] Kacan, E, Ulgen, K. *Energy analysis of Solar Combisystems in Turkey*. Energy Conversion and Management. 2012;64:378-86.

[18] Leconte, A., Achard, G., Papillon, P. *Global approach test improvement using a neural network model identification to characterise solar combisystem performances*. Solar Energy, 2012; 86(7):2001-2016.

[19] Sterling, S.J., Collins, M.R. *Feasibility analysis of an indirect heat pump assisted solar domestic hot water system*. Applied Energy. 2012;93:11-7.

[20] Deng, S., Dai, Y.J., Wang, R.Z. Matsuura T, Yasui Y. *Comparison study on performance of a hybrid solar-assisted CO2 heat pump*. Applied Thermal Engineering. 2011;31:3696-705.

[21] Kjellsson, E., Hellström, G., Perers, B. *Optimization of systems with the combination of ground-source heat pump and solar collectors in dwellings*. Energy. 2010;35:2667-73.

[22] Lundh, M., Zass, K., Wilhelms, C., Vajen, K., Jordan, U. *Influence of store dimensions and auxiliary volume configuration on the performance of medium-sized solar combisystems*. Solar Energy. 2010;84:1095-102.

[23] Thür, A. *Compact solar combisystem*. Diss. Ph. D. thesis, report R-160, Department of Civil Engineering, Technical University of Denmark, 2007.

[24] Spur, R., Fiala, D., Nevrala, D., Probert, D. *Influence of the domestic hot-water daily draw-off profile on the performance of a hot-water store*. Applied Energy. 2006;83:749-73.

[25] Andersen, E., Furbo, S. *Investigations of solar combisystems*. ISES Solar World Congress 2005 Proceedings, Orlando, Florida.

[26] Lund, P.D. *Sizing and applicability considerations of solar combisystems*. Solar Energy. 2005;78:59.

[27] Andersen, E., Shah, L.J., Furbo, S. *Thermal Performance of Danish Solar Combi Systems in Practice and in Theory*. Journal of solar energy engineering. 2004;126:744-9.

[28] Weiss, Werner W. *Solar heating systems for houses: a design handbook for solar combisystems*. Earthscan, 2003.

[29] Jordan, U., Vajen, K. *Influence of the DHW profile on the Fractional Energy Savings - A Case Study of a Solar Combisystem*. Solar Energy. 2001;69(6): 197-08.

[30] Hadorn, J. C. *Solar and Heat Pump Systems for Residential Buildings*. Wiley; 2015 (in press).

[31] Klein, A., Beckman, A., Mitchell, W., Duffie, A. *TRNSYS 17–a transient system simulation program. Madison*. Solar Energy Laboratory, University of Wisconsin; 2011.

[32] MacSheep. *MacSheep - New Materials and Control for a next generation of compact combined Solar and heat pump systems with boosted energetic and exergetic performance*, European Union's Seventh Framework Programme project, 2012-2015. (http://www.macsheep.spf.ch/) accessed on 2015-05-25.

[33] Dott, R., Haller, M.Y., Ruschenburg, J., Ochs, F., Bony, J. *The Reference Framework for System Simulations of the IEA SHC Task 44 / HPP Annex 38 - Part B: Buildings and Space Heat Load* – A techinical report of subtask C, Report C1 Part B, Paris. (http://task44.iea-shc.org/data/sites/1/publications/T44A38_Rep_C1_B_ReferenceBuildingDescription_Final_Revised_130906.pdf ) accessed on 2015-05-25.

[34] Bales, C., Betak, J., Broum, M., Chèze, D., Cuvillier, G., Haberl, R., Hafner, B., Haller, M.Y., Hamp, Q., Heinz, A., Hengel, F., Kruck, A., Matuska, T., Mojic,I., Petrak, J., Poppi, S., Sedlar, J., Sourek, B., Thissen, B., Weidinger, A. *Optimized solar and heat pump systems*, *components and dimensioning - Deliverable 7.3* - MacSheep report. (http://www.macsheep.spf.ch/Reports-Deliverables.245.0.html2015) accessed on 2015-05-25.

[35] Kaçan, E. *Exergetic optimization of basic system components for maximizing exergetic efficiency of solar combisystems by using response surface methodology*. Energy and Buildings, 2015; 91: 65-82.

[36] Data set for Viessmann Vitosol 200F, Planungsanleitung, A. Viessamann Deutschland GmbH, Germany, 2011. (http://www.viessmann.de/de/ein-_zweifamilienhaus/produkte/Solarthermie/Vitosol_200-F.html ) Data accessed on 2015-03-09.

[37] Data set for Viessmann Vitocell 340-M/360-M , Datenblatt, A. Viessamann Deutschland GmbH, Germany, 2013. (http://www.viessmann.de/content/dam/internet-global/pdf_documents/Datenblaetter_2013/WWB/DB-5368782_05-2013.pdf ) Data accessed on 2015-03-09.

[38] Technical guide for Viessmann Vitocal 200-S, A. Viessamann Deutschland GmbH, Germany, 2010.

(http://www.viessmann.de/content/dam/internet-global/pdf_documents/Datenblaetter_2013/EV/5811525_05-2013_DE.pdf ) Data accessed on 2015-03-09.

[39] Haller, M.Y., Perers, B., Bales, C., Paavilainen, J., Dalibard, A., Fischer, S., Bertram, E. *TRNSYS Type 832 v5. 00 „Dynamic Collector Model by Bengt Perers ": Updated Input-Output Reference*. 2012.

[40] Drück, H., Pauschinger, T. *MULTIPORT Store-Model Type 340*; 2006.

[41] EN 12977-3:2008. *Thermal solar systems and components. Custom built systems Performance test methods for solar water heater stores*.

[42] Haller, M.Y., Mojic, I., Frank, E., Kaufmann, M., Lötscher, L., Podhradsky, J., Huggenberger, A., Boller, S., Meier, B. *Disturbance of stratification caused by direct horizontal inlets into a water storage tank*. Proc. of the EuroSun 2014 Conference, Aix-les-Bains, France.

[43] Heinz, A., Haller, M.Y., 2012. *Appendix A3-Description of TRNSYS Type 877 by IWT and SPF. Models of Sub-Components and Validation for the IEA SHC Task*.

[44] prEN 12977-2:2007. *Thermal Solar Systems and Components - Custom Built Systems - Part 2: Test methods for solar water heaters and combisystems.*